Acceleration feedback control on an AT

B. Sedghi[a] and B. Bauvir [a] and M. Dimmler[a]

[a]European Southern Observatory (ESO), Karl-Schwarzschild-Strasse. 2, Garching, Germany

ABSTRACT

The VLT observatory operated by ESO is located on Cerro Paranal in Chile and consists of four identical 8-m telescopes and four 1.8-m VLTI Auxiliary telescopes (ATs). In order to further improve the tracking axes performance of telescopes regarding wind rejection, different control techniques have been evaluated.

Ongoing investigation and studies show that by measuring the acceleration and using that in an appropriate control strategy the performance of telescope tracking in face of external perturbation can be improved. The acceleration signal contains the non filtered information (advanced phase compared to velocity and position) of the perturbation load, e.g. wind load. As a result the reaction of the control is faster and hence the perturbation rejection is more efficient. In this paper, two acceleration feedback techniques are discussed and the results of the measurement test on an AT telescope are presented.

Keywords: Acceleration feedback, telescope axes control, perturbation rejection, wind buffeting

1. INTRODUCTION

At the beginning of 2007 a test campaign was realized on one of the Auxiliary telescopes (AT4)[1] to test, evaluate and demonstrate two acceleration feedback control (AFC) techniques on tracking performance of the telescope mount system. The purpose was to use acceleration measurements in addition to velocity and position to improve the perturbation rejection property of the servo loops. The main idea behind the approach is that the acceleration signal contains the non filtered information of the perturbation load. By using an appropriate control strategy the reaction to the perturbations is faster and hence the performance can be improved.

During the test campaign two different AFC strategies were investigated and implemented:

i) acceleration loop based on internal model principle (estimating the effect of perturbation using a model of the system),

ii) cascade acceleration feedback loop (proportional gain controller plus a low-pass filter).

For both methods the frequency response of the telescope altitude axis was measured and a parametric model for controller design was identified.

In a series of ESO technical reports detailed results were documented. This paper gives a summary of the results.

In the first part of this paper, the perturbation rejection properties of two techniques are presented. They are compared with the classical cascade velocity and position loop control scheme. In the second part, measurement results of the test campaign are presented. The observations are discussed and the pros and cons of the techniques are enumerated.

2. ACCELERATION FEEDBACK CONTROL: PERTURBATION REJECTION PROPERTY

In this section, the perturbation rejection properties of a classical cascade velocity and position loop scheme are presented. The main axes control of a telescope generally follows the same scheme. Next, the two AFC techniques are briefly introduced and their perturbation rejection properties are presented and compared to the classical schema. The noise propagation of the accelerometer is neglected. Here, the objective is to compare the external load perturbation rejection properties regardless of the measurement noise. Later in Section 3.3 this issue will be elaborated.

Further author information: (Send correspondence to B. Sedghi)
B. Sedghi: E-mail: bsedghi@eso.org, Telephone: +49 89 32006529

2.1. Velocity and Position control

Consider the control scheme of the main axes of a telescope (Figure 1) consisting of two velocity (tacho) and position (encoder) feedback loops. Let $G_v = G_a/s$ * be the transfer function of the telescope axis drive to velocity, C_v the velocity loop controller, and C_p the position loop controller. The telescope is perturbed by the external load (wind), let $H_v = H_a/s$ be the open loop transfer function from wind load, w, to tacho v.

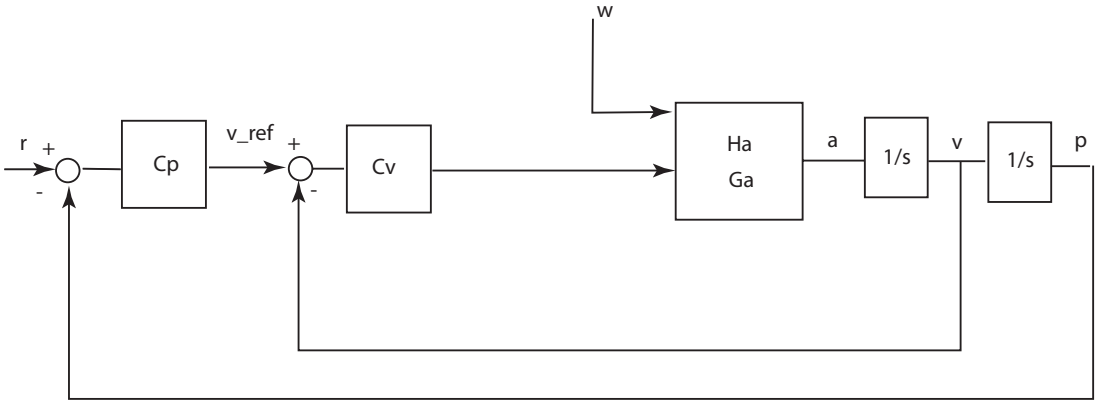

Figure 1. Velocity and position feedback loop scheme

The closed-loop velocity is given by:

$$v = w\frac{H_v}{1+C_vG_v} + v_{ref}\frac{C_vG_v}{1+C_vG_v} \tag{1}$$

Let $T_v = \dfrac{C_vG_v}{1+C_vG_v}$ and $S_v = \dfrac{1}{1+C_vG_v}$, then the encoder reading p is given by

$$p = \frac{1}{s}S_vH_vw + v_{ref}\frac{1}{s}T_v \tag{2}$$

The velocity reference v_{ref} in closed loop is given by: $v_{ref} = C_p(r-p)$ where r is the position reference. By replacing the above equation in Eq. (2) the position in closed-loop can be derived:

$$\begin{aligned} p &= \frac{1}{s}S_vH_vw + C_p(r-p)\frac{1}{s}T_v \\ p &= H_pS_vS_pw + S_pC_p\frac{1}{s}T_vr \end{aligned} \tag{3}$$

where $S_p = \dfrac{1}{(1+C_p\frac{1}{s}T_v)}$ and $H_p = \frac{1}{s}H_v$. Let W_{PSD} be the PSD of the wind load w. From the above equation the power spectral density (PSD) of the axis position, P_{PSD} is given by:

$$P_{PSD} = |H_pS_vS_p|^2W_{PSD} \tag{4}$$

As it can be seen from the above equation the performance of altitude axis is driven by two sensitivity functions namely S_v (velocity loop) and S_p (position loop). By designing appropriate controllers these functions are minimized in frequency range where the perturbation load is large. Note that since the control scheme is in a cascade structure, the inner-loop should be much faster (higher bandwidth) than the outer loop. This means that the perturbation rejection is mainly dominated by the velocity loop S_v.

* $\frac{1}{s}$ stands for integral operator

2.2. Cascade AFC

Figure 2 shows the control scheme with an additional acceleration loop in a cascade structure (cascade AFC).

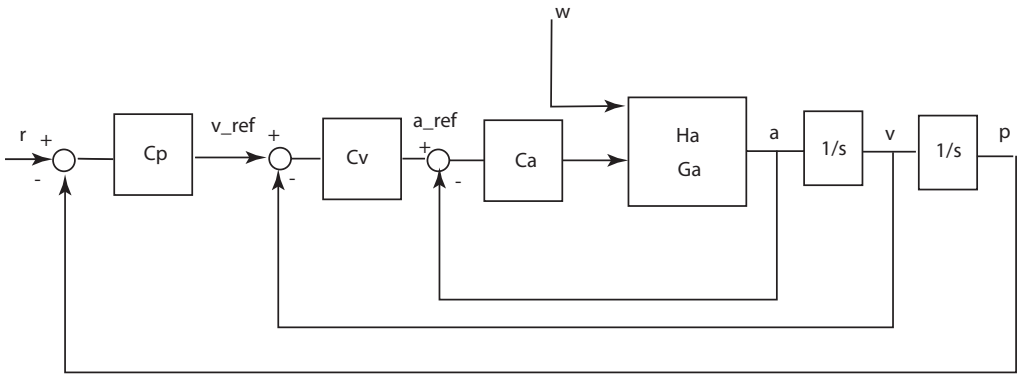

Figure 2. Cascade AFC scheme

Let G_a be the transfer function from the axis drive torque to the acceleration and H_a from wind load to acceleration. Define C_a as the acceleration loop controller then the closed-loop acceleration, a is given by

$$a = \frac{H_a}{1 + C_a G_a} w + a_{ref} \frac{C_a G_a}{1 + C_a G_a} \tag{5}$$

The velocity is then

$$v = \frac{1}{s} \frac{H_a}{1 + C_a G_a} w + a_{ref} \frac{1}{s} \frac{C_a G_a}{1 + C_a G_a} \tag{6}$$

where a_{ref} is defined by $a_{ref} = C_v(v_{ref} - v)$. Then

$$\begin{aligned} v &= \frac{H_v w}{1 + C_a G_a} + C_v(v_{ref} - v) \frac{1}{s} \frac{C_a G_a}{1 + C_a G_a} \\ v &= S_a \bar{S}_v H_v w + v_{ref} \bar{T}_v \end{aligned} \tag{7}$$

where $\bar{G}_v = \frac{1}{s} \frac{C_a G_a}{1 + C_a G_a}$, $S_a = \frac{1}{1 + C_a G_a}$, $\bar{S}_v = \frac{1}{1 + C_v \bar{G}_v}$, and $\bar{T}_v = \frac{C_v \bar{G}_v}{1 + C_v \bar{G}_v}$.

Following the same lines of Section 2.1 it can be shown that the closed-loop position is given by:

$$p = H_p S_a \bar{S}_v S_p w + S_p C_p \frac{1}{s} \bar{T}_v r \tag{8}$$

where $S_p = \frac{1}{(1 + C_p \frac{1}{s} \bar{T}_v)}$. The position (encoder) PSD is given by

$$P_{PSD} = |H_p S_a \bar{S}_v S_p|^2 W_{PSD} \tag{9}$$

As it can be seen and by comparing the definition to the classical scheme (Eq. 4) the acceleration rejection transfer function S_a is added to the rejection capability of the servo system, hence improving the performance against the perturbation load. This property can be explained alternatively:

At steady state (constant velocity reference) the acceleration of telescope is proportional to the wind load and the inverse of inertia of the axis, i.e. $a = w(\frac{1}{J})$. The acceleration loop with a control gain of $C_a = k_a$ leads

to an increase of the inertia against the perturbation that is $a = w(\frac{1}{J + k_a})$. In addition, it is known that with the acceleration loop damping of the modes can be increased.[2] The outcome of this property is the possibility of increasing the bandwidth of the velocity and position loops which consequently leads to a better perturbation rejection.

2.3. Plug-in module AFC

Contrary to classical AFC approaches where acceleration is fed back in a nested loop (cascade), in the internal model approach the acceleration signal is used to estimate the perturbation load. The control command consists of two components: one is the velocity feedback and the other is the inverse of the estimated wind load. The design follows the approach (a plug-in acceleration control module) presented in.[3]

Figure 3 shows the control scheme with velocity and position loops including the AFC plug-in module.

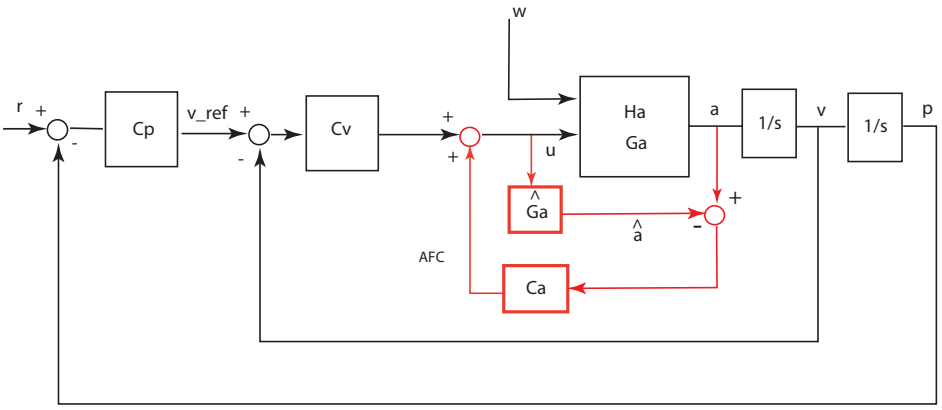

Figure 3. Velocity and position feedback loop with AFC plug-in module

For the sake of simplicity of the demonstration assume $H_a = G_a$. It can be shown that the velocity transfer function using the AFC plug-in module is given by:

$$v = S_v H_v w + S_v H_v \big(C_a(a - \hat{a})\big) + v_{ref} T_v$$
$$v = S_v H_v w + S_v H_v \big(C_a(G_a u + G_a w - \hat{G}_a u)\big) + v_{ref} T_v$$

and for $\hat{G}_a = G_a$:

$$v = (1 - C_a G_a) S_v H_v w + v_{ref} T_v \tag{10}$$

where C_a is the acceleration controller and G_a is the acceleration transfer function from the drive torque to the altitude axis acceleration. Let $S_{afc} = (1 - C_a G_a) S_v$, then using the similar calculation procedure used earlier the encoder closed-loop transfer function can be calculated as:

$$p = H_p S_{afc} S_p w + S_p C_p \frac{1}{s} T_v r \tag{11}$$

The PSD of encoder in this case is given by

$$P_{PSD} = |H_p S_{afc} S_p|^2 W_{PSD} \tag{12}$$

Since the Plug-in AFC module does not change the dynamics of the closed-loop velocity transfer function then the position loop controller will remain unchanged and thus S_p remains unchanged. This means that the position

and velocity loops can be designed independently from the acceleration loop. The acceleration controller can be 'plugged-in' to the existing velocity and position controller without changing the stability conditions. In terms of perturbation rejection, however the velocity sensitivity transfer function is modified $S_{afc} = (1 - C_a G_a) S_v$. To reduce the effect of perturbation C_a should be designed to minimize the rejection transfer function in the frequency range of interest. Typically, the error is reduced be minimizing $||W_a(1 - C_a G_a)||_\infty$, where W_a specifies the frequency range where the function should be minimized. In[3] a robust design for C_a is proposed, where C_a is parameterized as pseudo inverse of G_a in terms of closed-loop inversion, i.e. $C_a = \frac{N}{1 + N G_a}$. The new controller N should be designed such that in desired frequencies $|C_a G_a| \simeq 1$.

3. MEASUREMENT TEST RESULTS ON THE AUXILIARY TELESCOPE (AT4)

A pair of Wilcoxon accelerometer is installed (glued and clamped) on the tube of the AT4 telescope near the center piece. The accelerometers are installed in face of each other and in the plane, including M1, which creates 90 degree angle with the altitude axis (see Figure 4). This way the differential reading of each pair of accelerometers will give information on rotation of the tube around the axis.

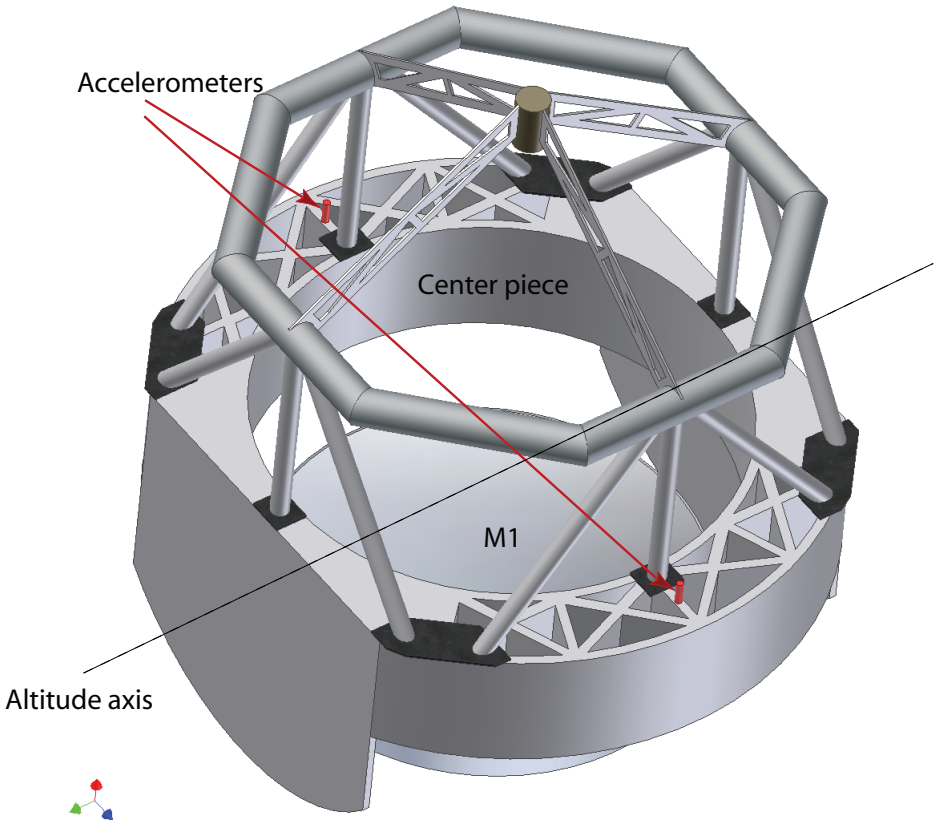

Figure 4. AT4 tube structure: location of Wilcoxon accelerometers

During the test campaign using a spectral analyzer various frequency responses of the altitude axis in closed-loop velocity configuration were measured.

The closed-loop frequency responses from velocity reference and drive torque to tacho (velocity) and accelerometer were measured. In this case the open-loop torque to velocity and accelerometer frequency responses

were derived. In addition, the velocity sensitivity responses S_v were measured. Using an optimization procedure parametric models of the altitude axis for designing the servo controllers were derived.

For velocity loop a PID controller with 2 notch filters and a low pass filter was designed. Figure 5 shows the measured open-loop together with the identified parametric model frequency response, the measured velocity closed-loop frequency response, and the response obtained from the model.

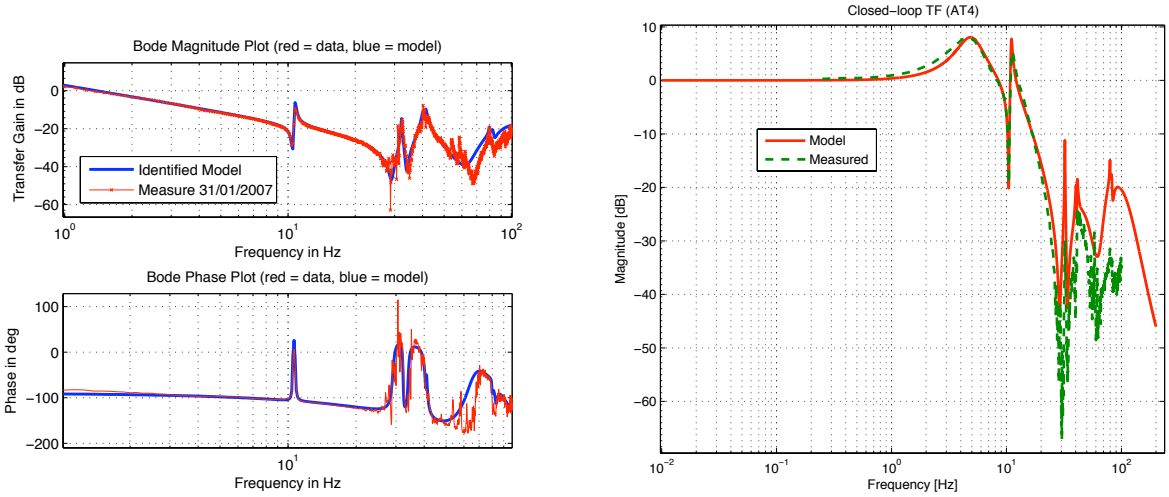

Figure 5. AT4 altitude axis: Open loop (velocity/torque) and closed-loop frequency responses (measured vs. identified model)

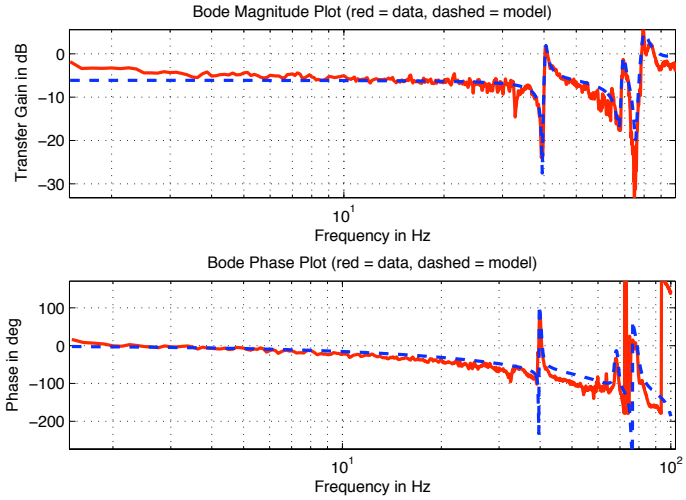

Figure 6. Acceleration frequency response (measured vs. identified model)

Using the signal analyzer the frequency responses from the altitude axis drive and the 'differential' acceleration (difference of two accelerometer readings) were measured. Based on the measurements a parametric model $\hat{G}_a$ was identified. Figure 6 shows the frequency response of the measured acceleration together with the identified model. This model was used to design the acceleration loop controller in cascade AFC approach. For the plug-in

AFC approach, since the low frequency range of acceleration was in interest and in this range the frequency response was nearly constant, the estimated model was selected to be $\hat{G}_a = 0.5$.

3.1. Cascade AFC

The telescope real-time software environment was modified in order to be able to implement the cascade AFC control. The control scheme was set as presented in Figure 2.

The acceleration loop controller was chosen to be a low pass filter and a gain, i.e. $C_a = \dfrac{k_a \alpha}{s+\alpha}$. Figure 7 shows the measured velocity loop frequency response after including the acceleration loop (compare with the velocity frequency response without acceleration loop).

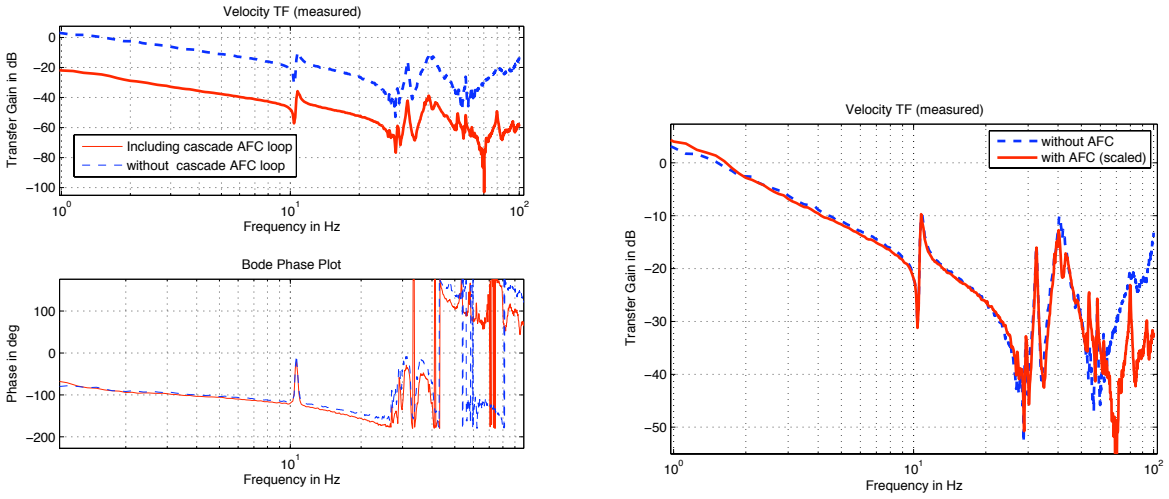

Figure 7. AT4 altitude axis: measured open loop (velocity/torque) frequency response (without AFC vs. cascade AFC)

As it was expected and explained earlier, the response including the inner acceleration loop is shifted down compared to the case where no AFC is applied (increase of inertia). In addition to this effect, which is only a scaling on the gain of the velocity transfer function, the high frequency modes are as well attenuated (see the right image of Figure 7). Therefore the design of the controller would be less affected by these modes (possibility of increasing the control bandwidth). Based on the identified model, including the AFC loop, a new velocity loop controller was designed (PI controller with a notch filter). Figure 8 shows the measured sensitivity responses compared to the response of the system without a cascade AFC loop.

Figure 9 (left) shows the measured frequency response from wind load to position encoder comparing the results with default controller and when cascade AFC is implemented. To have an idea of the temporal behavior a sinusoidal perturbation signal with frequency of 5 Hz was injected in the telescope drive and the amplitude of the residual error on the tacho (velocity measurements) was compared to the case where no cascade AFC was implemented. Figure 9 (right) shows that the cascade AFC module reduces the amplitude of the error signal.

Filtering a Von Karman wind load PSD model † by the measured disturbance transfer function of the default and cascade AFC approach yields to a RMS tracking error ratio $\dfrac{e_{p_{AFC}}}{e_p} = 0.51$ (an improvement by a factor of 2 in image jitter compared to the case without cascade AFC).

†Model with following parameters: Turbulence intensity: 0.16, mean wind torque 100[Nm], Outer scale of turbulence: 20[m], mean wind speed: 10[m/s], area: 4[m^2] and conversion factor from Nm to volt being 98.6

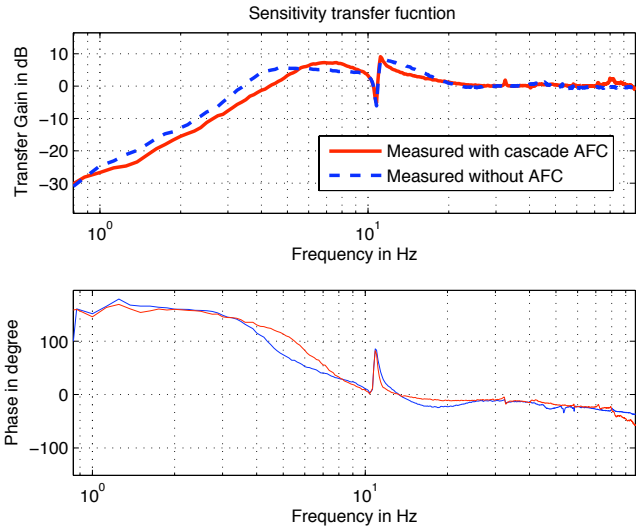

Figure 8. AT4 altitude axis: measured velocity loop sensitivity response (No AFC vs. cascade AFC)

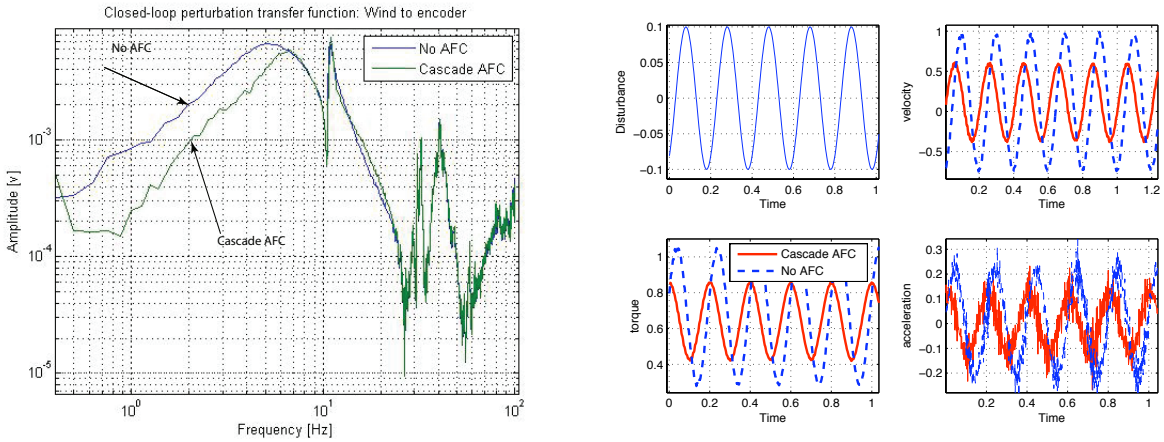

Figure 9. Left: Wind load torque to position encoder response (No AFC vs. cascade AFC). Right: Measured responses to sinusoidal disturbance at 5Hz (No AFC vs. cascade AFC)

3.2. Plug-in module AFC

The internal model AFC (plug-in) module was implemented on telescope control system. The AFC module is composed of two high and low-pass and notch filters two eliminate the drift and high frequency noise of the accelerometer. The acceleration model used in the module was chosen to be $\hat{G_a} = 0.5$. As usual the closed-loop and sensitivity frequency responses on the altitude axis were measured. Figure 10 shows the responses [‡] for AFC plug-in being off and on.

As predicted the Plug-in module does not change the closed-loop behavior of the system, which again shows that the module can be put on and off without changing the closed-loop properties of the system (redesigning of the velocity and position loops are not needed). There is a slight mismatch between two measured responses

[‡]the frequency measurement measurement conducted had low signal to noise ratio below 1Hz this is the reason for relativelybad quality of the curve at these frequencies

which is mainly due to the mismatch of the acceleration model in the plug-in module and the real acceleration measurements[§]. On the other hand the rejection function is clearly improved at lower frequencies (up to 10Hz).

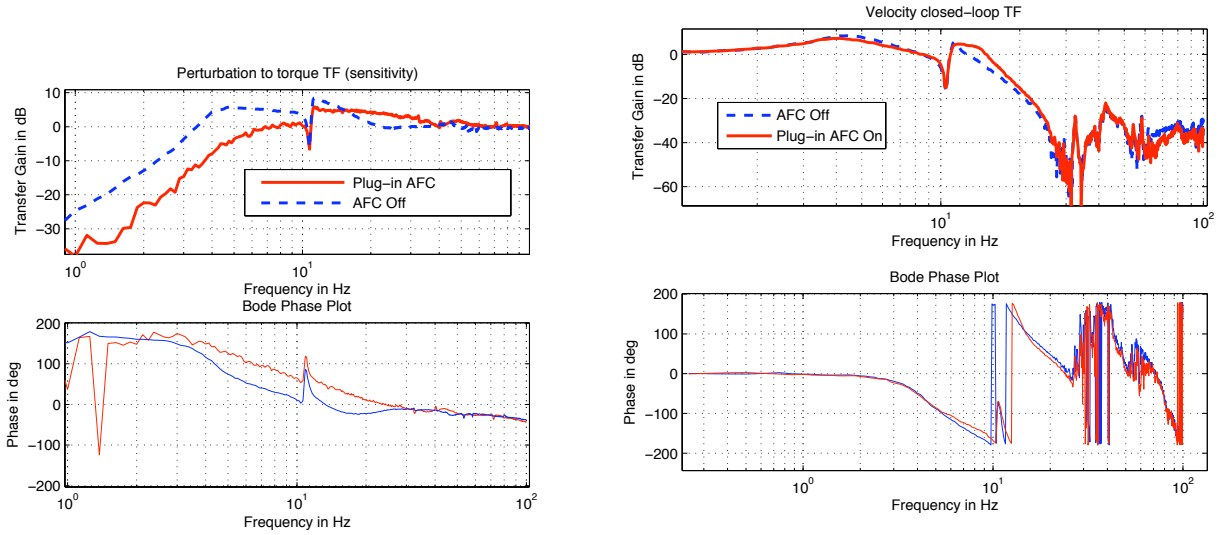

Figure 10. Left: Measured velocity loop sensitivity response (No AFC vs. AFC plug-in). Right: measured velocity loop closed-loop frequency response.

Figure 11 (left) shows the measured frequency response from wind load to position encoder comparing the results with default controller and when the plug-in AFC module is implemented. To have an idea of the temporal behavior a sinusoidal perturbation signal with frequency of 5Hz was injected to the system and the amplitude of the residual error on tacho (velocity measurements) was compared with the case without plug-in AFC. Figure 11 (right) shows the AFC plug-in module decrease the amplitude of the error signal.

Filtering a Von Karman wind load PSD model by the measured disturbance transfer function of the default and plug-in AFC approach yields to a RMS tracking error ratio $\frac{e_{pAFC}}{e_p} = 0.31$ (an improvement by a factor of 3 in image jitter compared to the case where AFC plug-in is off).

[§]In the case of difference between the estimated acceleration response and the real response, it can be shown that the closed-loop transfer function is modified by $\delta_a = \frac{C_a}{1 - C_a\Delta}$ where $\Delta = G_a - \hat{G}_a$, i.e. $\bar{T} = \frac{\delta_a C_v G_v}{1 + \delta_a C_v G_v}$

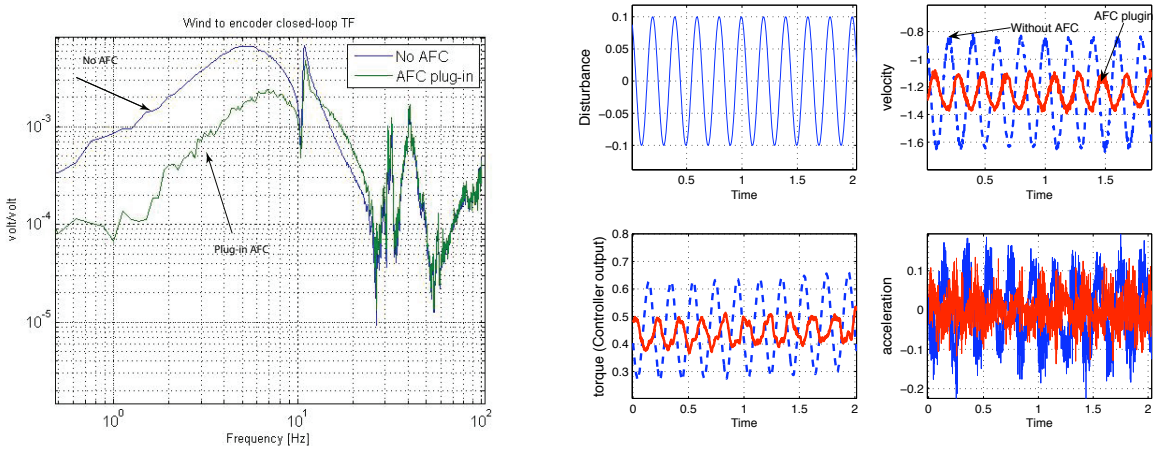

Figure 11. Left: Wind load torque to position encoder response (No AFC vs. plug-in AFC). Right: Measured responses to sinsusoidal disturbance at 5Hz (No AFC vs. cascade AFC).

3.3. Open Dome test and noise propagation

During the period of tests (8 nights) the wind velocity was very low (average 3 to 4 m/s). The open dome measurements were performed once when the wind speed reached 5 m/s. The telescope was first performed tracking without AFC (cascade and plug-in) and the performance was close to the resolution of the altitude axis position encoder. The system was performing at the level that one could not expect any improvement by including the AFC modules. By turning on the AFC it was observed that the performance is getting worst by observing high level noise on tacho readings. The reason was the propagation of the accelerometer noise through the control loops.

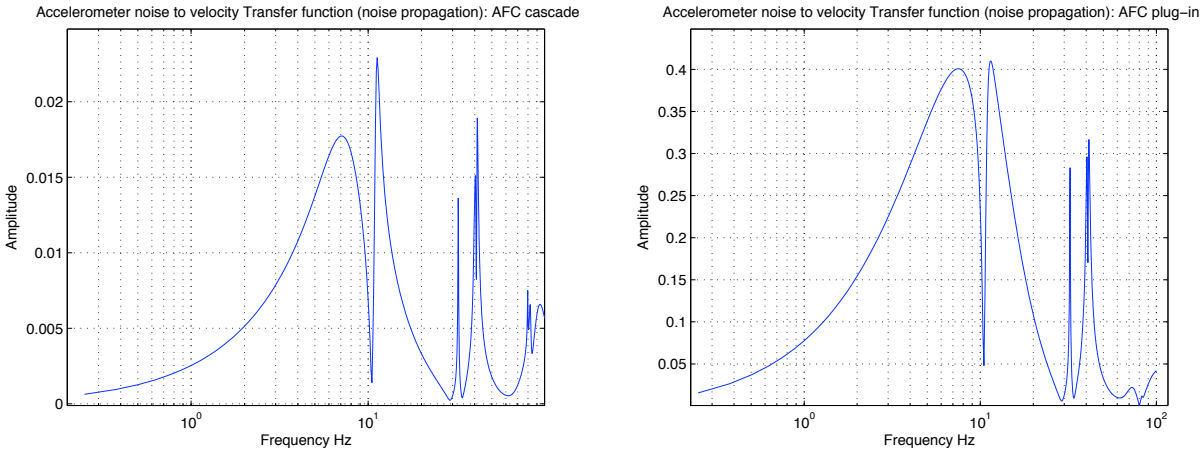

Figure 12. Accelerometer noise to velocity (tacho) transfer function Left: cascade AFC, Right: plug-in AFC

To see how the sensor noise is propagated in the case of two AFC approaches the transfer functions from noise to velocity of the altitude axis are derived. It can be shown that in the case of cascade AFC the transfer function from sensor noise, n_a to velocity, v, is given by $\frac{v}{n_a} = -\frac{\bar{G}_v}{1 + C_v \bar{G}_v}$, and in the case of plug-in AFC is

given by $\frac{v}{n_a} = \frac{G_v C_a}{1 + C_v G_v}$. The frequency responses for these two cases are shown in Figure 12.

It can be seen that in the case of plug-in AFC the amplitude of noise transfer function is much higher (factor of 20!) than that of the cascade AFC. This shows that the approach is more sensitive to the choice of accelerometer and its noise specification. The effect can be seen by comparing the level of the noise in the time responses shown in Figures 9 and 11. The same effect was as well observed when the telescope dome was open with practically no wind load. The encoder reading was much more noisier in the case of plug-in AFC than with the cascade technique.

As no time was left to optimize and change the design of the controllers, it was decided to measure the PSD of the accelerometer in the case of closed dome and telescope in off mode. The PSD of accelerometer shows several resonant peaks caused by the telescope structure (high sensitivity of the accelerometer to the vibration sources). Figure 13 shows the PSD of the accelerometer before and after adding a low-pass filter plus several notches at resonant frequencies.

The filtered acceleration signal was once used for AFC plug-in approach which was more sensitive to the sensor noise. In this case the same parameters of the controller were used (no optimization for new filtered acceleration signal was performed). The sinusoidal perturbation test was repeated and it was observed that the level of the noise was reduced in the responses (see Figure 13 right).

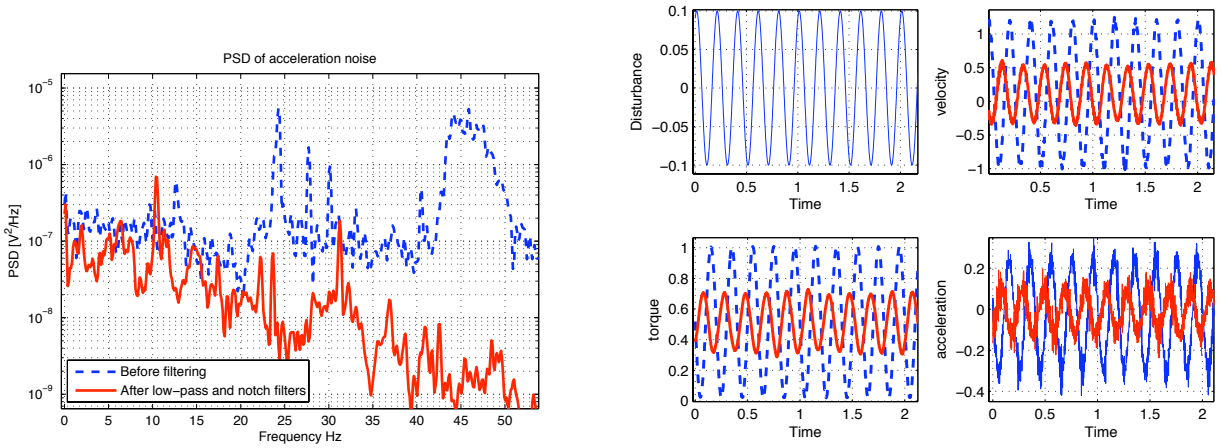

Figure 13. Left: PSD of accelerometer measurements before and after filtering. Right: Response to sinusoidal disturbance at 5 Hz using filtered acceleration signal (No AFC vs. AFC plug-in)

The performance can be improved by an appropriate filtering of the acceleration signal (low-pass filtering is appropriate for wind load which has its energy mainly at low range frequencies), however this requires more care and attention and should be investigated in future works.

4. CONCLUSIONS

During the test period it was demonstrated that the acceleration measurements accompanied with an appropriate control strategy can improve the perturbation rejection property of the telescope axis. Either the plug-in controller or cascade showed an improvement at frequencies up to the first resonant frequency of the axis. This was measured directly by injecting a large band perturbation signal on the axis. The pros and cons of each approach and the general impression after the test period are summarized as following:

- Cascade AFC: the technique showed as well its capability to improve the perturbation rejection property of the control system. The improvement up to factor two in low frequencies was observed. In addition

to improving the disturbance rejection property (S_a is included), the approach has another important advantage: it adds roll-off and damping to mechanical modes. This makes the design of the velocity loop controller relatively easier with a better robustness property. The disadvantage is that every time a parameter in the acceleration control loop is changed the velocity loop controller needs to be re-tuned.

- Plug-in AFC: The approach is very promising. With a careful design of the controller the sensitivity function can be decreased in the frequency range of interest (by a factor of 3 for the given wind load profile). As the name itself suggests the approach does not change the stability requirement of the system, so the closed-loop behavior of system (tracking) stays untouched. The module can be turn on-off without any consequence. The main drawback with the approach is the high level accelerometer noise propagation (higher than for the cascade approach). Filtering the measurements can solve the problem to some extent, however careful a selection of the accelerometers is mandatory. The accelerometers should have a good signal/noise ratio and sensitivity in the frequency range of interest (high frequency acceleration measurements are not needed for the application where wind loads should be attenuated).

REFERENCES

1. B. Koehler, M. Kraus, J. M. Moresmau, K. Wirenstrand, R. K. P. Duhoux, L.Andolfato, and F. Gonte, "The VLTI auxiliary telescopes: measured performances" in advances in stellar interferometry," *Proceedings of SPIE Vol. 6268 (SPIE, Bellingham, WA 2006)* (626841), 2006.
2. A. Preumont, *Vibration Conrtrol of active structures, an introduction*, Kluwer academic publishers, 2nd Edition, 2002.
3. A. Babinski and T. Tsao, "Acceleration feedback design for voice coil actuated direct drive," *Proc. American Control Conference* , pp. 3713–3717, 1999.